A New Extraction Method for the Two-Parameter FET Temperature Noise Model

Mikael Garcia, Jörgen Stenarson, *Student Member, IEEE,* Klas Yhland, Herbert Zirath, *Member, IEEE,* and Ilcho Angelov, *Member, IEEE*

***Abstract*—This paper presents a direct extraction method for the associated noise temperatures T_d and T_g in the field-effect transistor (FET) temperature noise model. The method is related to nodal analysis of circuits. T_d and T_g are extracted from the small-signal model parameters and the noise parameters of the device. It is also theoretically shown that there exist source admittances that cancel the thermal noise contribution at the output from either T_d or T_g in the model. Finally, a commercially available GaAs pseudomorphic high electron-mobility transistor (pHEMT) is measured and modeled for a wide range of bias points. Comparisons between measured and modeled noise parameters are presented in the 2–26-GHz frequency range.**

***Index Terms*— FET noise model, nodal analysis, noise-model extraction, source balance admittance.**

I. Introduction

The field-effect transistor (FET) temperature noise model, first proposed in 1988 by Pospieszalski [1]–[2], has been widely accepted as an easy-to-use and powerful FET noise model. Pospieszalski showed that the high-frequency noise from FET chips can be modeled as thermal noise in a small-signal equivalent circuit. Depending on the device characteristics and application, the model is either used as a single-parameter (T_d), two-parameter (T_d, T_g), or three-parameter (T_d, T_g, T_p) model [1]–[5]. In the single-parameter model, the associated gate noise temperature T_g is set to the ambient temperature. Since T_g is typically a very weak function of the drain current, this model is sufficient for applications at low or medium–high drain currents [6]. The three-parameter model is intended for analysis of devices that suffer from significant gate–current leakage. In this case, the parameter T_p is the associated noise temperature of an additional intrinsic gate–source resistor that accounts for the gate–current leakage in the Schottky contact. However, for devices with a nonleaky gate contact, the original two-parameter model is adequate at both cryogenic and room temperatures [1], [2].

Manuscript received October 27, 1997; revised April 14, 1998.

M. Garcia, J. Stenarson, K. Yhland, and I. Angelov are with the Department of Microwave Technology, Chalmers University of Technology, S-412 96 Göteborg, Sweden (e-mail: garcia@ep.chalmers.se).

H. Zirath is with the Department of Microwave Technology, Chalmers University, S-412 96 Göteborg, Sweden, and also with Ericsson Microwave System, S-431 84 Mölndal, Sweden.

Publisher Item Identifier S 0018-9480(98)08029-6.

Associated with every model, there should always be an extraction procedure to obtain the parameter values. A disadvantage of many models is the lack of a rational extraction method. Compared with the field of small-signal model extraction, the field of noise-model extraction is less developed. In discussing noise models, the extraction procedure is often simply explained as "matrix operations." This explanation is often coupled with a reference to the general theory of correlation matrices by Hillbrand and Russer [7]. Consequently, all essential details needed in the extraction of the parameter values are omitted. Most users prefer explicit extraction formulas, which can be applied directly. Recently, a straightforward extraction formula was presented for use in direct extractions of the single-parameter FET temperature noise model [8]. However, direct extraction formulas for the two-parameter model have never been reported.

In this paper, a new parameter-extraction method is proposed for the two-parameter FET temperature noise model. The model parameters are extracted from measured noise parameters and the element values in the small-signal equivalent circuit. Also, the concept of source-admittance balance in the FET temperature noise model is introduced. Finally, measured and modeled noise parameters are compared for a commercially available GaAs pseudomorphic high electron-mobility transistor (pHEMT) in the 2–26-GHz frequency range.

II. The Extraction Method

Basically, there are two methods for directly calculating the two parameters in the FET temperature noise model. First, the parameters can be calculated from noise figures measured at two different frequencies, using the same source admittance. However, sensitivity problems occur if the selected frequencies are too close to one another. Measurement errors then dominate the actual difference in the measured noise figures. Again, choosing these frequencies far apart complicates studies of the frequency dependence in the model parameters. On the other hand, no source tuner is needed in the measurement setup. The second approach is to calculate the parameters from noise figures measured for two different source admittances, with the frequency held constant. The major drawback with this method is the need of a source tuner. However, commercial noise-parameter test sets used for noise characterizations always include a source tuner. Consequently, if a source tuner is available, the latter method is superior since it is less sensitive

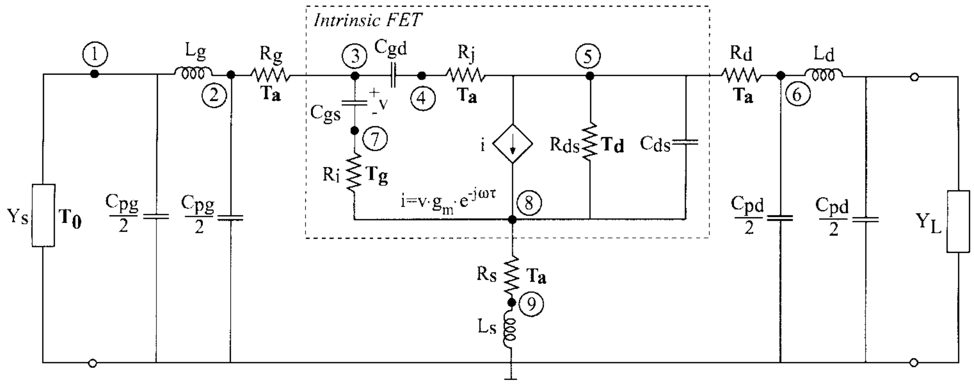

Fig. 1. The broad-band small-signal equivalent circuit used in the FET temperature noise model, together with the external source and load admittances. The node numbers used in this paper are encircled.

to measurement errors. Therefore, this latter method was selected in this paper.

A. Arbitrary Selections of Source Admittances

The broad-band small-signal equivalent circuit used for the FET chip is shown in Fig. 1. The encircled numbers (1–9) are the node numbers used in this paper. According to (8), in [8] the noise figure F of this FET model can be written as

$$F(Y_s) = 1 + a_0(Y_s) + a_1(Y_s)T_d + a_2(Y_s)T_g \tag{1}$$

where Y_s is the source admittance

$$\begin{aligned} a_0(Y_s) = &\frac{T_a}{T_0\,\mathrm{Re}(Y_s)|Z_{6,1}|^2} \\ &\cdot\left(\frac{|Z_{6,2}-Z_{6,3}|^2}{R_g} + \frac{|Z_{6,4}-Z_{6,5}|^2}{R_j}\right. \\ &\left. + \frac{|Z_{6,5}-Z_{6,6}|^2}{R_d} + \frac{|Z_{6,8}-Z_{6,9}|^2}{R_s}\right) \end{aligned} \tag{2}$$

$$a_1(Y_s) = \frac{|Z_{6,5}-Z_{6,8}|^2}{R_{\mathrm{ds}}T_0\,\mathrm{Re}(Y_s)|Z_{6,1}|^2} \tag{3}$$

$$a_2(Y_s) = \frac{|Z_{6,7}-Z_{6,8}|^2}{R_i T_0\,\mathrm{Re}(Y_s)|Z_{6,1}|^2} \tag{4}$$

T_a is the ambient temperature, and $Z_{i,j}$ are elements of the nodal impedance matrix. The source temperature T_0 is the standard noise temperature (290 K) defined in [9]. Furthermore, the nodal impedance matrix $\mathbf{Z}$ for this circuit is given by

$$\mathbf{Z} = \begin{bmatrix} Z_{1,1} & \cdots & Z_{1,9} \\ \cdots & \cdots & \cdots \\ Z_{9,1} & \cdots & Z_{9,9} \end{bmatrix} = \begin{bmatrix} Y_{1,1} & \cdots & Y_{1,9} \\ \cdots & \cdots & \cdots \\ Y_{9,1} & \cdots & Y_{9,9} \end{bmatrix}^{-1} \tag{5}$$

and (6), shown at the bottom of this page. All other admittance matrix elements are identical and zero.

Note that the noise figure of this circuit is, by definition, independent of C_{pd}, L_d, and Y_L. Thus, node 6 can be used as the output node in the analysis.

In this paper, we assume that the noise parameters are available. Consequently, the device noise figure can be calculated for a given source admittance. A system of two linear equations is obtained from (1) if noise figures for two different source admittances are calculated. That is,

$$F(Y_{s1}) = 1 + a_0(Y_{s1}) + a_1(Y_{s1})T_d + a_s(Y_{s1})T_g \tag{7}$$

$$\left.\begin{array}{lll}
Y_{1,1} = Y_s + \dfrac{1}{j\omega L_g} + j\omega\dfrac{C_{pg}}{2} & Y_{1,2} = Y_{2,1} = -\dfrac{1}{j\omega L_g} & Y_{5,7} = Y_{8,3} = -g_m e^{-j\omega\tau} \\
Y_{2,2} = \dfrac{1}{R_g} + j\omega\dfrac{C_{pg}}{2} + \dfrac{1}{j\omega L_g} & Y_{2,3} = Y_{3,2} = -\dfrac{1}{R_g} & Y_{7,8} = -\dfrac{1}{R_i} \\
Y_{3,3} = j\omega(C_{\mathrm{gd}} + C_{\mathrm{gs}}) + \dfrac{1}{R_g} & Y_{3,4} = Y_{4,3} = -j\omega C_{\mathrm{gd}} & Y_{8,7} = -\dfrac{1}{R_i} + g_m e^{-j\omega\tau} \\
Y_{4,4} = \dfrac{1}{R_j} + j\omega C_{\mathrm{gd}} & Y_{3,7} = Y_{7,3} = -j\omega C_{\mathrm{gs}} & \\
Y_{5,5} = \dfrac{1}{R_{\mathrm{ds}}} + \dfrac{1}{R_d} + \dfrac{1}{R_j} + j\omega C_{\mathrm{ds}} & Y_{4,5} = Y_{5,4} = -\dfrac{1}{R_j} & \\
Y_{6,6} = \dfrac{1}{R_d} & Y_{5,6} = Y_{6,5} = -\dfrac{1}{R_d} & \\
Y_{7,7} = j\omega C_{\mathrm{gs}} + \dfrac{1}{R_i} & Y_{5,8} = Y_{8,5} = -j\omega C_{\mathrm{ds}} - \dfrac{1}{R_{\mathrm{ds}}} & \\
Y_{8,8} = \dfrac{1}{R_s} + \dfrac{1}{R_i} + \dfrac{1}{R_{\mathrm{ds}}} + j\omega C_{\mathrm{ds}} & Y_{8,9} = Y_{9,8} = -\dfrac{1}{R_s} & \\
Y_{9,9} = \dfrac{1}{j\omega L_s} + \dfrac{1}{R_s} & Y_{5,3} = g_m e^{-j\omega\tau} &
\end{array}\right\} \tag{6}$$

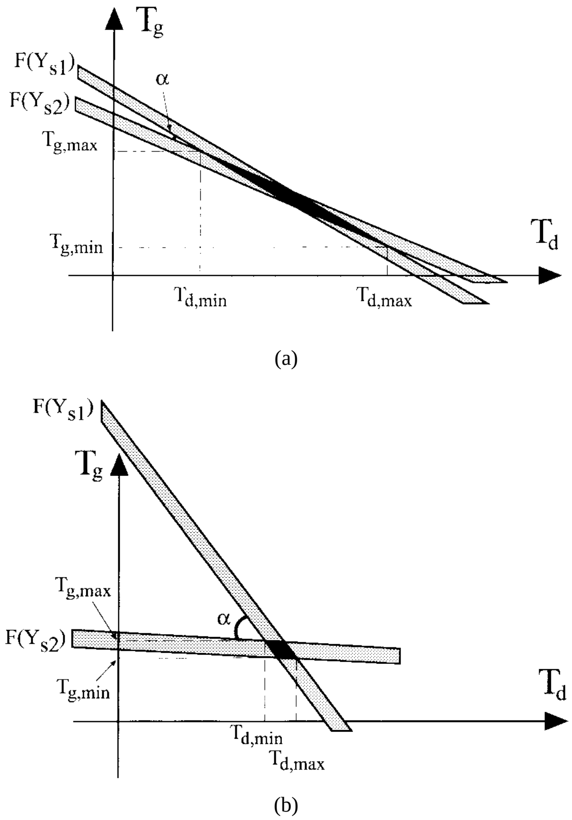

Fig. 2. Graphical representations of (7) and (8) for two different selections of Y_{s1} and Y_{s2}. (a) Selection I. (b) Selection II.

and

$$F(Y_{s2}) = 1 + a_0(Y_{s2}) + a_1(Y_{s2})T_d + a_2(Y_{s2})T_g. \quad (8)$$

Finally, the solution to this system of linear equations gives the associated noise temperatures T_d and T_g.

B. Balanced Selections of Source Admittances

The accuracy of the extracted T_d and T_g is ultimately determined by the accuracy in the measurements. However, it is important to note that the selection of the two source admittances Y_{s1} and Y_{s2} affect the sensitivity to measurement errors in the extraction. In Fig. 2, (7) and (8) are presented graphically for two different selections of Y_{s1} and Y_{s2}. The measurement error, here represented as an uncertainty in the noise figure, implies linear zones rather than linear lines for the $T_g(T_d)$ dependence. If α (the intercept angle between the linear zones) is increased, the accuracy in the estimation of T_g and T_d is increased, as shown in Fig. 2(b). A practical condition for selecting Y_{s1} and Y_{s2} is the following: one zone is parallel to the T_g axis and the other is parallel to the T_d axis. Since the axes are orthogonal, T_d and T_g can be extracted independently. According to (1), this selection corresponds to one source admittance satisfying

$$a_1(Y_s) = 0 \quad (9)$$

and the other satisfying

$$a_2(Y_s) = 0. \quad (10)$$

However, (3) and (4) give

$$a_1(Y_s) = 0 \Leftrightarrow Z_{6,5} = Z_{6,8}$$
$$a_2(Y_s) = 0 \Leftrightarrow Z_{6,7} = Z_{6,8}. \quad (11)$$

The elements of the nodal impedance matrix $\mathbf{Z}$ are given by the cofactor method and (5) as

$$Z_{6,5} = (-1)^{6+5}\frac{\det \mathbf{A}_{5,6}}{\det \mathbf{Y}} = -\frac{\det \mathbf{A}_{5,6}}{\det \mathbf{Y}}$$
$$Z_{6,7} = (-1)^{6+7}\frac{\det \mathbf{A}_{7,6}}{\det \mathbf{Y}} = -\frac{\det \mathbf{A}_{7,6}}{\det \mathbf{Y}}$$
$$Z_{6,8} = (-1)^{6+8}\frac{\det \mathbf{A}_{8,6}}{\det \mathbf{Y}} = \frac{\det \mathbf{A}_{8,6}}{\det \mathbf{Y}} \quad (12)$$

where $\mathbf{A}_{i,j}$ is the submatrix formed by deleting the ith row and jth column of $\mathbf{Y}$.

According to (6) and the fact that the determinant is a multilinear function, the minors of $\mathbf{Y}$ in (12) can be written as

$$\det \mathbf{A}_{5,6} = \det \mathbf{A}_{5,6}|_{Y_s=0} + (-1)^{1+1}Y_s \det(\mathbf{A}_{5,6})_{1,1}$$
$$\det \mathbf{A}_{7,6} = \det \mathbf{A}_{7,6}|_{Y_s=0} + (-1)^{1+1}Y_s \det(\mathbf{A}_{7,6})_{1,1}$$
$$\det \mathbf{A}_{8,6} = \det \mathbf{A}_{8,6}|_{Y_s=0} + (-1)^{1+1}Y_s \det(\mathbf{A}_{8,6})_{1,1} \quad (13)$$

where $(\mathbf{A}_{ij})_{n,m}$ is the submatrix formed by first deleting the ith row and the jth column of $\mathbf{Y}$ and then deleting the nth row and the mth column of the remaining matrix. By combining (11)–(13), one gets

$$a_1(Y_s) = 0 \Leftrightarrow Y_s = Y_{sd} = -\frac{\det \mathbf{A}_{5,6}|_{Y_s=0} + \det \mathbf{A}_{8,6}|_{Y_s=0}}{\det(\mathbf{A}_{5,6})_{1,1} + \det(\mathbf{A}_{8,6})_{1,1}} \quad (14)$$

and

$$a_2(Y_s) = 0 \Leftrightarrow Y_s = Y_{sg} = -\frac{\det \mathbf{A}_{7,6}|_{Y_s=0} + \det \mathbf{A}_{8,6}|_{Y_s=0}}{\det(\mathbf{A}_{7,6})_{1,1} + \det(\mathbf{A}_{8,6})_{1,1}}. \quad (15)$$

Note that when the source admittance is equal to $Y_{\rm sg}$ the model noise figure is independent of T_g. Similarly, the noise figure is independent of T_d if the source admittance equals $Y_{\rm sd}$. The explanation for this independence is that these source admittances balance the equivalent circuit at the output (so that the thermal noise generated by either T_d or T_g is canceled).

Finally, the associated noise temperatures T_d and T_g are given by (1), (14), and (15) as

$$T_d = \frac{F(Y_{\rm sg}) - 1 - a_0(Y_{\rm sg})}{a_1(Y_{\rm sg})} \quad (16)$$

and

$$T_g = \frac{F(Y_{\rm sd}) - 1 - a_0(Y_{\rm sd})}{a_2(Y_{\rm sd})}. \quad (17)$$

Consequently, T_d and T_g can be extracted separately if the source balance admittances $Y_{\rm sg}$ and $Y_{\rm sd}$ are known.

TABLE I
EXTRACTED SMALL-SIGNAL MODEL PARAMETERS FOR THE NE 32500 pHEMT. PARASITICS: $C_{\mathrm{pg}} = C_{\mathrm{pd}} = 11.6$ fF, $L_g = 49.1$ pH, $L_s = 2.5$ pH, $L_d = 39.5$ pH, $R_g = 0.5\ \Omega$, $R_s = 1.9\ \Omega$, $R_d = 2.9\ \Omega$. ($I_{\mathrm{ds,sat}} = 90$ mA)

V_{ds} [V]	I_{ds} [mA]	C_{gs} [fF]	C_{gd} [fF]	C_{ds} [fF]	g_m [mS]	Tau [ps]	R_i [Ω]	R_j [Ω]	R_{ds} [Ω]
2.0	5.0	109	24.8	48.9	48.4	0.7	4.1	0.0 *	221
2.0	10.0	130	22.6	51.9	72.5	0.6	3.3	0.0 *	157
2.0	15.0	142	20.8	53.8	87.9	0.4	3.1	0.0 *	134
2.0	20.0	148	20.7	54.2	98.3	0.4	2.8	0.0 *	122
2.0	25.0	151	19.6	55.3	105	0.4	2.6	0.0 *	116
2.0	30.0	151	19.1	56.3	109	0.4	2.5	0.0 *	111
2.0	35.0	152	19.0	56.2	110	0.4	2.7	0.0 *	109
2.0	40.0	151	18.3	56.5	108	0.5	2.8	0.0 *	107
2.0	45.0	152	18.3	56.8	104	0.5	2.3	0.0 *	106
2.0	50.0	152	17.9	56.4	99.1	0.3	2.1	0.0 *	105
2.0	55.0	151	17.8	55.8	88.0	0.5	2.2	0.0 *	106

* Note that if any of the resistances in the equivalent circuit equals zero, there is a potential risk for numerical problems. Consequently, R_j was set to 1 μΩ.

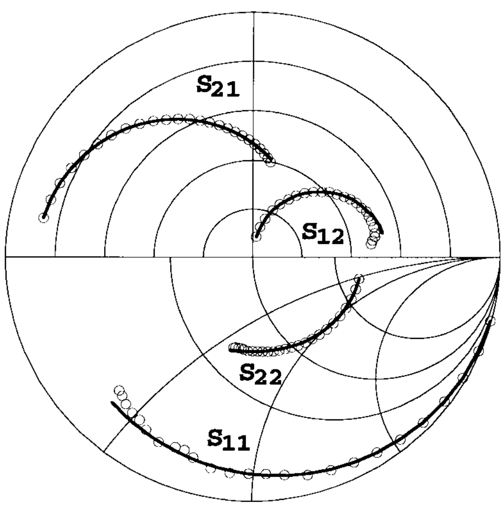

Fig. 3. Measured (◯) and modeled (—) S-parameters for the NEC device in the 2–26-GHz frequency range at $V_{\mathrm{ds}} = 2.0$ V and $I_{\mathrm{ds}} = 55$ mA. The S_{21} and S_{12} radii are 6.0 and 0.2, respectively. The model parameters are listed in Table I.

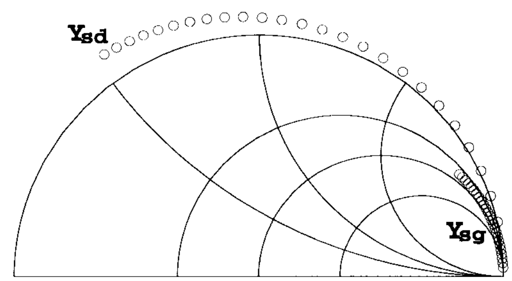

Fig. 4. Calculated source balance admittances Y_{sg} and Y_{sd} for the NEC device in the 2–26-GHz frequency range at $V_{\mathrm{ds}} = 2.0$ V and $I_{\mathrm{ds}} = 55$ mA. The model parameters are listed in Table I.

III. EXPERIMENTAL RESULTS

A commercially available low-noise GaAs pHEMT (NEC NE 32500) was measured on-wafer using an ATN NP5B wafer probe noise-parameter test set. Noise parameters as well as S-parameters were measured in the 2–26-GHz frequency range. The direct extraction method presented in [10] and [11] was used for the extraction of the small-signal model parameters. The results obtained for the NE 32500 chip are listed in Table I. In Fig. 3, measured and modeled S-parameters are compared at $V_{\mathrm{ds}} = 2.0$ V and $I_{\mathrm{ds}} = 55$ mA.

Equations (14) and (15) were then used for the calculation of the source balance admittances Y_{sg} and Y_{sd}. The results are presented in Fig. 4. Thereafter, the corresponding noise figures $F(Y_{\mathrm{sg}})$ and $F(Y_{\mathrm{sd}})$ were calculated from the measured noise parameters. The associated noise temperatures T_d and T_g were then finally calculated using (16) and (17). For comparison, the single-parameter model was also extracted. In this model, T_g is set to the ambient temperature. The drain temperature T_d was extracted directly from 50-Ω noise figures calculated from the measured noise parameters. In Fig. 5, the extracted noise temperatures are presented in the 2–26-GHz frequency range at $V_{\mathrm{ds}} = 2$ V and $I_{\mathrm{ds}} = 55$ mA. It is clear that T_g is significantly higher than the ambient temperature at this bias. Furthermore, in Fig. 6, the extracted noise temperatures are presented as a function of drain current. A dashed line is added at the 290-K level. The results show that T_g equals the ambient temperature at drain currents lower than 20 mA. For comparisons between $T_d^{(1)}$ and $T_d^{(2)}$, one should keep in

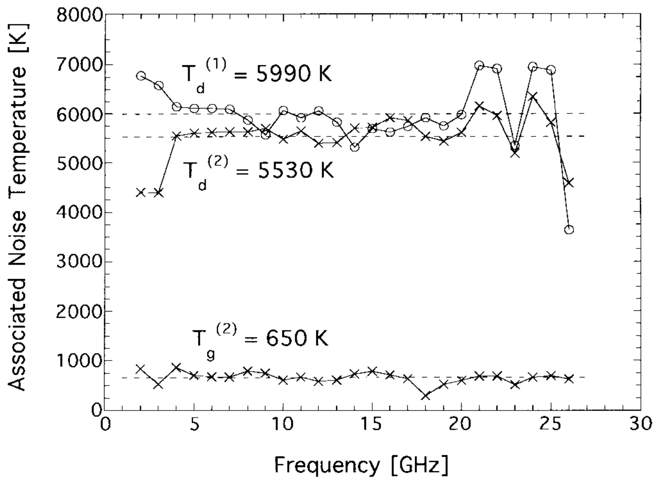

Fig. 5. Extracted gate and drain noise temperatures T_g and T_d versus frequency for the NEC device at $V_{\rm ds} = 2.0$ V and $I_{\rm ds} = 55$ mA. The single-parameter model ($T_g = T_a$): $T_d^{(1)}$, and the two-parameter model: $T_g^{(2)}$ and $T_d^{(2)}$. The dashed lines represent the mean values. $T_a = 290$ K.

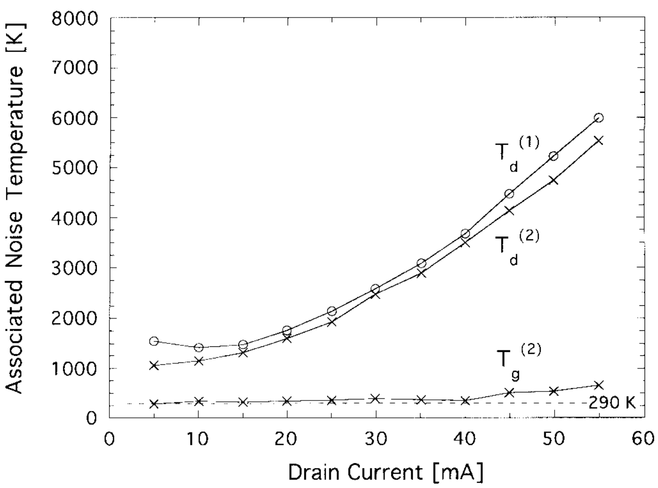

Fig. 6. Extracted gate and drain noise temperatures T_g and T_d versus drain current for the NEC device at $V_{\rm ds} = 2.0$ V. The single-parameter model ($T_g = T_a$): $T_d^{(1)}$, and the two-parameter model: $T_g^{(2)}$ and $T_d^{(2)}$. $T_a = 290$ K.

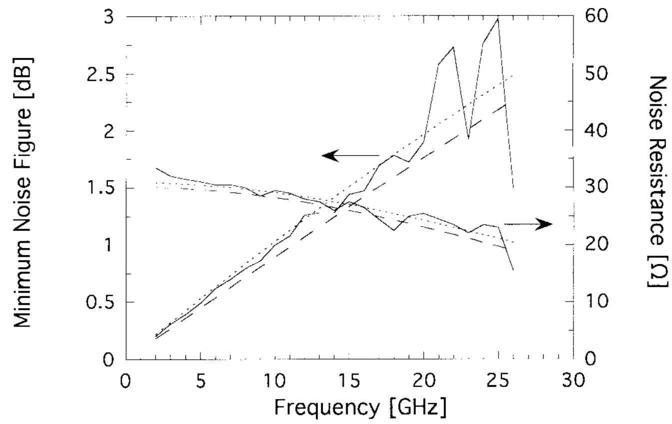

Fig. 7. Minimum noise figure $F_{\min}$ and noise resistance R_n versus frequency for the NEC device at $V_{\rm ds} = 2.0$ V and $I_{\rm ds} = 55$ mA. Measured data (—). Single-parameter model (– –): $T_d = 5990$ K and $T_g = T_a = 290$ K. Two-parameter model (··): $T_d = 5530$ K and $T_g = 650$ K.$T_a = 290$ K.

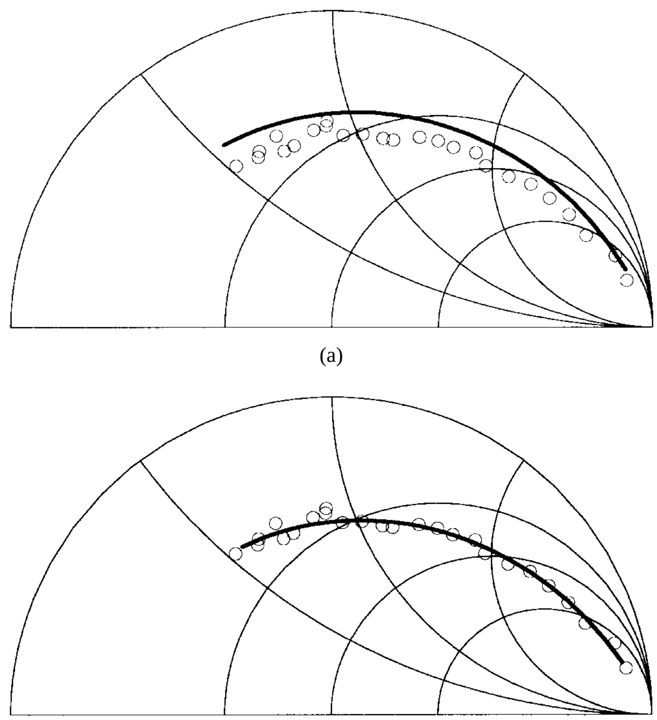

(a)

(b)

Fig. 8. Measured (◯) and modeled (—) optimal source reflection coefficient $\Gamma_{\rm opt}$ for the NEC device in the 2–26-GHz frequency range at $V_{\rm ds} = 2.0$ V and $I_{\rm ds} = 55$ mA. (a) Single-parameter model: $T_d = 5990$ K and $T_g = T_a = 290$ K. (b) Two-parameter model: $T_d = 5530$ K and $T_g = 650$ K. $T_a = 290$ K.

mind that $T_d^{(1)}$ is extracted here from the 50-Ω noise figure, while $T_d^{(2)}$ is extracted from the noise figure at the source balance admittance $Y_{\rm sg}$. Comparisons between measured and modeled (using the straightforward method recently proposed in [12]) noise parameters at $V_{\rm ds} = 2$ V and $I_{\rm ds} = 55$ mA are presented in Figs. 7 and 8. It is seen that at this high drain current bias ($I_{\rm ds} = 0.6 \cdot I_{\rm ds,\,sat}$) the two-parameter formulation is superior.

Finally, if T_d and T_g are to be calculated at source admittances other than $Y_{\rm sg}$ and $Y_{\rm sd}$, it is important to pay attention to the intercept angle α between the noise figure lines in the T_d–T_g plane (see Fig. 2). A small angle means that the extraction is very sensitive to measurement errors. The system admittance—20 mS—is often easy to realize in a measurement system. Consequently, from an experimental point of view, it can be interesting to use the system admittance as one of the two source admittances. The task is then to select the second admittance properly. In Fig. 9, the intercept angle is presented as a function of this second source admittance at $V_{\rm ds} = 2$ V and $I_{\rm ds} = 55$ mA. It can be seen that for low frequencies, only source admittances close to zero, i.e., open circuit, yield reasonable intercept angles [see Fig. 9(a)]. However, for higher frequencies, the area with acceptable intercept angles is significantly larger [see Fig. 9(b)]. Note that there is a valley close to $\Gamma_{\rm opt}$ at which the intercept angles are very small.

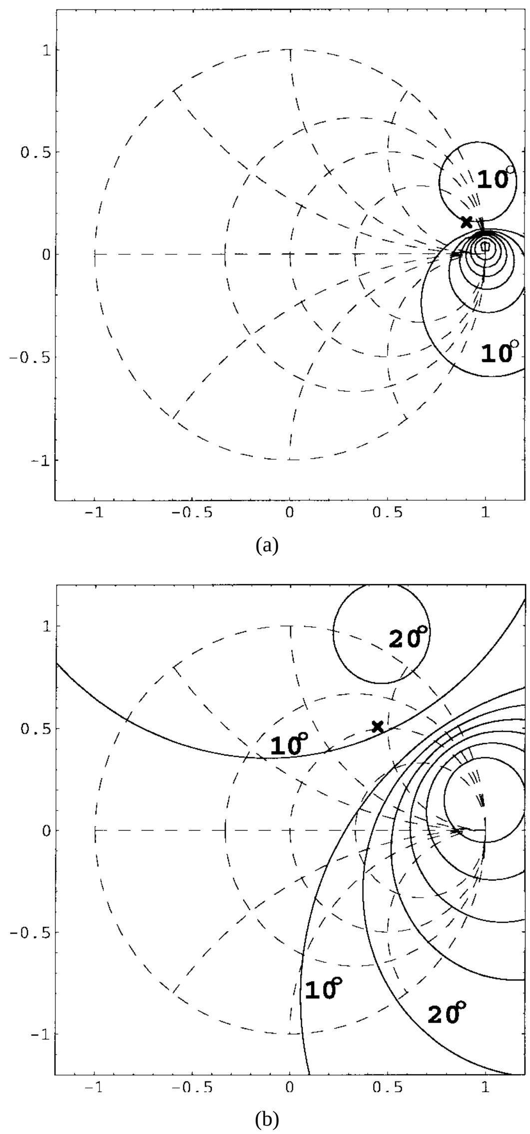

Fig. 9. The intercept angle α when $Y_{s1} = 20$ mS for the NEC device as a function of Y_{s2}. $V_{\rm ds} = 2.0$ V and $I_{\rm ds} = 55$ mA. A cross is used as a cursor for $\Gamma_{\rm opt}$. Contours are shown for every 10° between 0°–90°. (a) Frequency $= 2$ GHz. (b) Frequency $= 10$ GHz.

IV. Discussion and Conclusions

Direct extraction formulas for the calculation of the associated noise temperatures T_d and T_g in the FET temperature noise model have been reported. The formulas were derived for a broad-band small-signal equivalent circuit. As a result, the noise model is fully compatible with high-frequency small-signal FET models. The associated noise temperatures were calculated from the noise parameters and the element values in the small-signal equivalent circuit. To avoid high sensitivity to measurement errors, the two source balance admittances were used for the extraction of T_g and T_d. In this paper, the source balance admittances were only used in a computational procedure, together with the measured noise parameters. An alternative approach could be to extract T_g and T_d from noise figures actually measured at the source balance admittances. However, a problem with this method is that our experimental results show that the extracted small-signal model yields a source balance admittance $Y_{\rm sd}$ with a negative real part (see Fig. 4). As a result, the extraction of T_g using (17) becomes difficult. Another possibility is to extract T_d and T_g from noise figures measured at source admittances other than $Y_{\rm sd}$ and $Y_{\rm sg}$. For example, a set of the measured noise figures used by the noise test set for the calculation of the noise parameters can, for example, be used. However, access to these intermediate parameters can be restricted by the noise test-set software. The difficulty with this type of extraction is probably the selection of source admittances. Sensitivity problems occur if the intercept angle between the noise figure lines in the T_d–T_g plane is too small. For the case with the system admittance (20 mS) as one of the source admittances, it was shown that it can be difficult to tune for an admittance that corresponds to a large intercept angle.

Finally, the presented method was demonstrated on a commercially available GaAs pHEMT in the 2–26-GHz frequency range. The extracted noise models did compare well with the measured noise parameters. It should be pointed out that the proposed extraction procedure may run into computational problems at low frequencies. The reason for this is simply that it is numerically difficult to compute the impedance matrix at low frequencies for the equivalent circuit used in this paper. However, this is normally not a problem since the temperature noise model is only valid for frequencies where the flicker noise ($1/f$ noise) can be neglected. A study of the drain current dependence in the model parameters was also performed. It was shown that the associated gate noise temperature T_g was significantly higher than the ambient temperature at relatively high drain currents. A comparison between the single-parameter model (where T_g was set to the ambient temperature and T_d was extracted from the 50-Ω noise figure) and the two-parameter model also showed that at high drain currents, the best agreement with measured noise parameters was obtained with the two-parameter model.

Acknowledgment

The authors would like to thank Prof. E. Kollberg, Chalmers University of Technology, Göteborg, Sweden, for his support of this work. Dr. M. Pospieszalski, NRAO, Charlottesville, VA, is greatly acknowledged for fruitful discussions regarding this paper. Finally, special thanks go to Dr. H.-O. Vickes, Saab Ericsson Space, Mölndal, Sweden, for sharing the NEC devices.

References

[1] M. W. Pospieszalski, "A new approach to modeling of noise parameters of FET's and MODFET's and their frequency and temperature dependence," Nat. Radio Astronomy Observatory Electron. Div., Charlottesville, VA, Tech. Rep. 279, July 1988.
[2] ——, "Modeling of noise parameters of MESFET's and MODFET's and their frequency and temperature dependence," *IEEE Trans. Microwave Theory Tech.*, vol. 37, pp. 1340–1350, Sept. 1989.
[3] B. Hughes, "A temperature noise model for extrinsic FET's," *IEEE Trans. Microwave Theory Tech.*, vol. 40, pp. 1821–1832, Sept. 1992.
[4] M. W. Pospieszalski and W. J. Lakatosh, "Millimeter-wave cryogenically coolable amplifiers using AlInAs/GaInAs/InP HEMT's," in *IEEE MTT-S Dig.*, Atlanta, GA, 1993, pp. 515–518.
[5] R. Reuter, S. van Waasen, and F. J. Tegude, "A new noise model of HFET with special emphasis on gate leakage," *IEEE Electron Device Lett.*, vol. 16, pp. 74–76, Feb. 1995.

[6] M. W. Pospieszalski and A. C. Niedzwiecki, "FET noise model and on-wafer measurements of noise parameters," in *IEEE MTT-S Dig.*, Boston, MA, June 1991, pp. 1117–1120.
[7] H. Hillbrand and P. Russer, "An efficient method for computer-aided noise analysis of linear amplifier networks," *IEEE Trans. Circuits Syst.*, vol. CAS-23, pp. 235–238, Apr. 1976.
[8] M. Garcia, J. Stenarson, H. Zirath, and I. Angelov, "A direct extraction formula for the FET temperature noise model," *Microwave Opt. Technol. Lett.*, vol. 16, pp. 208–212, Nov. 1997.
[9] IRE Standards Committee, "IRE standards on electron tubes: Definitions of terms, 1962," *Proc. IEEE*, vol. 51, pp. 434–435, Mar. 1963.
[10] N. Rorsman, M. Garcia, C. Karlsson, and H. Zirath, "Accurate small-signal modeling of HFET's for millimeter-wave applications," *IEEE Trans. Microwave Theory Tech.*, vol. 44, pp. 432–437, Mar. 1996.
[11] M. Garcia, N. Rorsman, K. Yhland, H. Zirath, and I. Angelov, "Fast, automatic and accurate HFET small-signal characterization," *Microwave J.*, vol. 40, pp. 102–117, July 1997.
[12] M. Garcia, J. Stenarson, H. Zirath, and I. Angelov, "An algebraic method for noise parameter analysis of temperature noise models," *Microwave Opt. Technol. Lett.*, vol. 17, no. 5, pp. 287–291, Apr. 1998.

Mikael Garcia received the M.Sc. degree in electrical engineering and the Ph.D. degree in microwave electronics from Chalmers University of Technology, Göteborg, Sweden, in 1992 and 1998, respectively.

His current research interests are in the area of heterojunction FET (HFET) and MESFET modeling.

Jörgen Stenarson (S'98) received the M.Sc. degree in engineering physics from Chalmers University of Technology, Göteborg, Sweden, in 1997, and is currently working toward the Ph.D. degree.

His research is focused on FET noise models, noise-model extraction methods, and low-noise amplifier design.

Klas Yhland received the M.Sc. degree in electrical engineering from Lund University of Technology, Lund, Sweden, in 1992, and is currently working toward the Ph.D. degree at Chalmers University, Göteborg, Sweden.

From 1992 to 1994, he was with Ericsson Microwave Systems, Airborne Radar Division. In 1994, he joined the Microwave Electronics Laboratory, Chalmers University of Technology. His research interests are nonlinear FET circuits and device models for MESFET's and HFET's.

Herbert Zirath (S'84–M'86) received the M.Sc. degree in electrical engineering and the Ph.D. degree from Chalmers University of Technology, Göteborg, Sweden, in 1980 and 1986, respectively.

Since 1980, he has been a Researcher at Chalmers, where he is involved with cooled millimeter-wave Schottky diode mixers and properties of millimeter-wave Schottky barrier diodes. Since 1986, he has been responsible for the development of active millimeter-wave devices and MMIC-like InP and GaAs-based MESFET's and HEMT's, including their modeling and related circuits, such as active and resistive HEMT mixers, low-noise amplifiers, and harmonic generators for frequencies up to 120 GHz. In 1996, he became a Professor in the Department of Microwave Technology, Chalmers. Since 1995, he has been working part-time for Ericsson Microwave System, Mölndal, Sweden.

Ilcho Angelov (M'90) received the M.Sc. degree in electronics from the Moscow Electrical Institute, Moscow, Russia, in 1969, and the Ph.D. degree in physics and mathematics from Moscow State University, Moscow, Russia, in 1973.

Since 1976, he has worked with microwave oscillators and low-noise transistor amplifiers and receivers, including cryogenically cooled amplifiers. His recent research activity is in the field of HFET modeling and development of millimeter-wave HFET mixers and multipliers.